TECHNICAL MEMORANDUM

814

Evidence of a stratospheric methane bias in the IFS against MIPAS data

S. Massart, A. Agustí-Panareda, J. Flemming

Copernicus Department

October 18, 2017

European Centre for Medium-Range Weather Forecasts
Europäisches Zentrum für mittelfristige Wettervorhersage
Centre européen pour les prévisions météorologiques à moyen terme

Series: ECMWF Technical Memoranda

A full list of ECMWF Publications can be found on our web site under:
http://www.ecmwf.int/en/research/publications

Contact: library@ecmwf.int

European Centre for Medium-Range Weather Forecasts
Shinfield Park, Reading, RG2 9AX, England

Abstract

In this report, we compare simulated methane fields from the Integrated Forecasting System (IFS) with retrieved stratospheric methane profiles retrieved from the Michelson Interferometer for Passive Atmospheric Sounding (MIPAS). We assume that the used MIPAS retrieved methane profiles are the best estimate of the true atmospheric methane state in the stratosphere and we use them as the reference.

Simulated methane fields are provided by IFS in forecast mode with two different chemical mechanisms. Any differences between simulated methane and MIPAS retrievals could be attributed to following sources of error: (i) IFS transport, (ii) simplified methane chemistry, (iii) initial condition of the simulation, (iv) surface fluxes and (v) representativity error in the comparison. We believe that the representativity error (v) is of second order compared to the other errors. We also show that the initial condition (iii) is not the main driver of the difference.

The first main feature of the simulated methane from all experiments is an underestimation in the upper troposphere – lower stratosphere (UTLS) region where the tropopause acts like a barrier for the stratosphere – troposphere exchange. This underestimation of methane concentration in the model could be associated with a transport error (i) across the tropopause barrier or an underestimation in the tropospheric concentration linked with errors in surface fluxes (iv). This second hypothesis is nevertheless unlikely since the feature appears in simulations with different surface fluxes.

The second feature is a large underestimation around 10 hPa at high latitudes, stronger in the southern hemisphere during the summer season when the chemistry is the most active. This underestimation could be linked with (ii) errors in the methane chemical mechanisms. This is also the location of the surf zone where the planetary waves break in the winter, a phenomenon that could be at the origin of a descent of this methane-poor air-mass in the lower stratosphere after the summer season. This amplifies the methane underestimation in the UTLS.

The methane underestimation in the UTLS is opposite to the known overestimation of humidity, another tracer in the IFS. This humidity overestimation around 200 hPa, mainly in the summer hemisphere, produces a cold stratospheric bias persistent in the model. The stratospheric task force, an ECMWF cross-section initiative, aims to tackle this issue.

We demonstrate in this document that MIPAS methane retrievals therefore provide another insight of the model biases in various regions of the stratosphere. We claim that the model biases are likely linked to errors in the IFS transport (i) and to a less extend and more locally to an simplified methane chemistry in the IFS (ii). Methane simulations from IFS could be used to test various model configurations that impact the stratospheric transport and help improving the IFS stratospheric forecast in the future.

Contents

1 Introduction

The European Centre for Medium-Range Weather Forecasts (ECMWF) provides analyses and forecasts of the weather parameters from the surface up to the mesosphere. While the troposphere plays a major role in the medium-range weather, the stratosphere can also influence it. As an example, during stratospheric sudden warmings (SSW), the tropospheric forecasts can be sensitive to the stratospheric evolution on time-scales of 10 days (Mohanakumar, 2008).

The stratosphere of the ECMWF Integrated Forecasting System (IFS) may have attracted less attention than the troposphere since the introduction of stratospheric levels in the model. Understanding and improving the stratospheric forecast is nevertheless very much an ambition of ECMWF. A specific task force across ECMWF departments is currently in place with the objective to coordinate work on improving the IFS stratosphere (Polichtchouk *et al.*, 2017).

One source of variability of the stratosphere is the radiative heating rate. For example, short wave heating rate is dominated by ozone (O_3) while long wave cooling by water (H_2O), carbon dioxide (CO_2) and methane (CH_4). For that reason, the IFS includes climatological concentrations of the main radiatively active gases (O_3, CO_3, CH_4) based on the reanalysis of the Copernicus Atmosphere Monitoring Service (CAMS, `atmosphere.copernicus.eu`). Monge-Sanz *et al.* (2013) have tested the implementation of a methane parametrisation scheme in the IFS instead of the climatology. This scheme has been used to parametrise the sources of stratospheric water and the impact on the radiative forcing has been documented.

As part of CAMS the ability to transport chemical tracers within the IFS was developed. Methane is among the transported tracers. Apart from its role in radiative cooling and water vapour production, methane can provide helpful information on the model transport and particularly the stratospheric transport (sec. 2). This is this the property we are interested in for this report.

We compare simulated methane fields from the IFS with retrieved stratospheric methane profiles from the Michelson Interferometer for Passive Atmospheric Sounding (MIPAS, sec. 3). To investigate the influence of the methane chemical scheme, we used two methods to simulate methane chemistry in the stratosphere (sec. 4). The model–MIPAS comparison method is detailed in sec. 5. The MIPAS mission started in 2002 and ended in 2012. In this document we present and discuss the characteristics of the simulated methane fields versus MIPAS for the period from May 2008 to December 2010 or April 2012 depending on the configuration (sec. 6).

2 Stratospheric methane as a proxy for model transport

Methane is known to be third most important greenhouse gas in the atmosphere. Most of its mass is located in the troposphere where it plays a key role in tropospheric chemistry through oxidation by hydroxyl (OH) radicals and where it is an important source of carbon monoxide (CO). Methane is well-mixed in the troposphere as illustrated by two characteristics of the tropospheric methane profiles. First, the vertical mixing makes the vertical profile almost constant from the surface up to about 200 hPa (Fig. 1a). Second, the horizontal mixing makes the spatial and temporal variability around the average very small (Fig. 1b).

In the stratosphere the lifetime of methane is still long and its distribution is governed by chemical reactions and global circulation and mixing processes. The chemical reactions are mostly the oxidation by OH, the reaction with electronically excited atomic oxygen $O(^1D)$ and with chlorine (Cl), all resulting

in an increase of the methane loss rate with altitude (Fig. 1c). One consequence is the decrease of the methane concentration with altitude from the tropopause (around 100 to 200 hPa, Fig. 1a). The oxidation by OH is more active in the summer hemisphere in the polar region and to a less extend in the tropics as illustrated at 10 hPa, Fig. 2b. This distribution of the methane loss rate increases the spatio-temporal variability of methane around this altitude (Fig. 1b) and partially explains the strong horizontal gradients depicted Fig. 2a.

Methane stratospheric distribution is also determined by the global circulation and the mixing. The two main mixing regions for methane are the upper troposphere – lower stratosphere (UTLS) region and the surf zone induced by wave planetary breaking in the winter hemisphere around 10 hPa. These barriers enhance the gradients in the methane concentration and make stratospheric methane very sensitive to the transport. For these reasons, methane can provide helpful information on the model large scale stratospheric transport. Using methane as a tracer of model stratospheric transport requires nonetheless to have reliable observations to compare with.

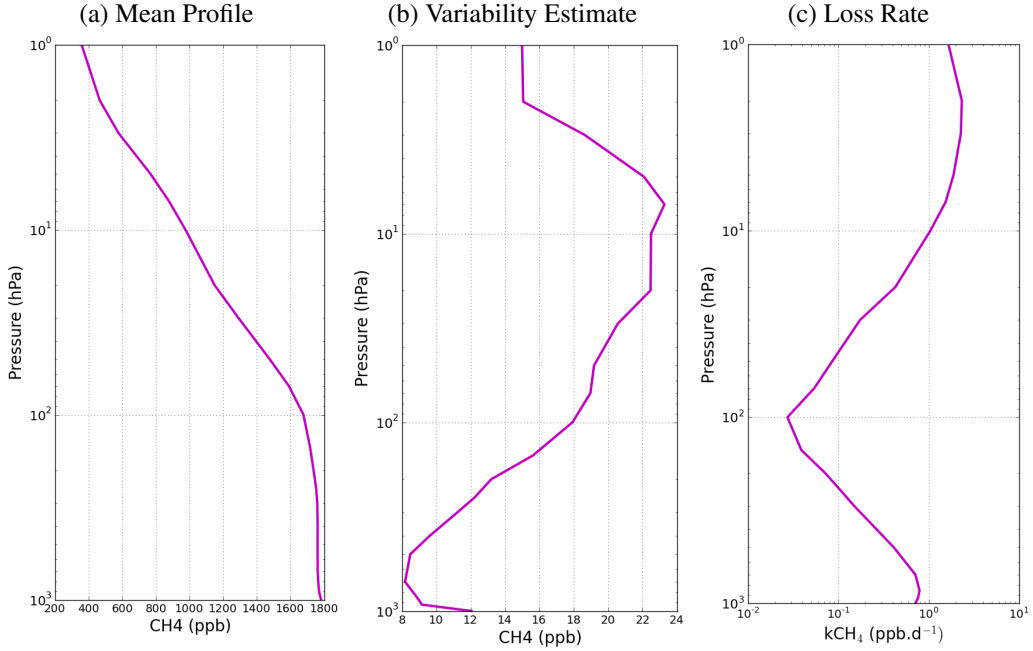

Figure 1: Methane global mean profile (left), estimation of the variability of the mean profile (middle) and global mean methane loss rate profile (right) from the CAMS near real time analysis between December 2015 and March 2016. The variability is estimated using the difference between the 48h and the 24h forecasts valid for the same date. The loss rate is based on climatological rates from Bergamaschi *et al.* (2009) times the model mean methane concentration.

3 Stratospheric methane observations

3.1 Availability of stratospheric methane observations

One could use methane profiles retrieved from three spatial instruments to monitor stratospheric methane simulated by a model. First, the Halogen Occultation Experiment (HALOE) that sampled methane profiles between 200 hPa and 0.01 hPa from 1991 to 2005. HALOE produced 30 high quality measurements

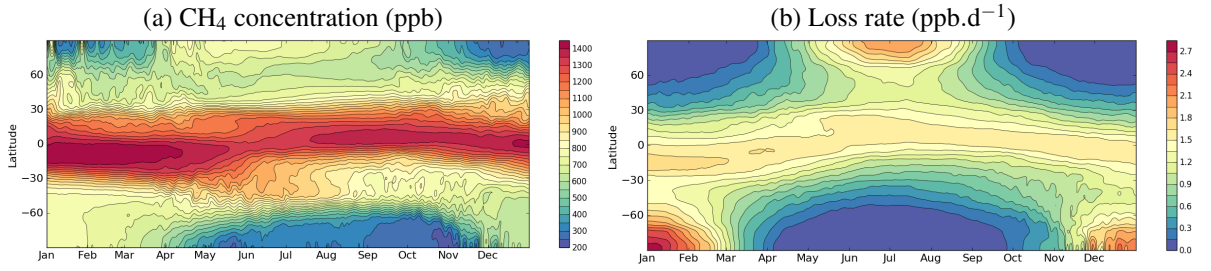

Figure 2: Time evolution of the zonal means of a the methane concentration and b the methane loss rate at 10 hPa for the year 2015 and from the CAMS near real time analysis. The loss rates is computed as the climatological rate from Bergamaschi *et al.* (2009) times the model methane concentration.

per day. Second, the Atmospheric Chemistry Experiment – Fourier Transform Spectrometer (ACE-FTS) that provides stratospheric methane profiles retrievals since 2003. The satellite carrying the ACE-FTS instrument has a circular high-inclination orbit, which results in a poor global coverage. The alternative is the Michelson Interferometer for Passive Atmospheric Sounding (MIPAS) that has a much better coverage than the two other instruments. On the other hand, covering the period between 2002 and 2012, the MIPAS mission is shorter than the ACE-FTS mission.

Apart from satellite retrievals, there are few measurements campaigns that sample the stratospheric profile of methane. As an example Membrive *et al.* (2016) compared IFS-based stratospheric methane profiles with AirCore-HR, an instrument flown on balloon-borne platforms. AirCore-HR provides methane vertical profiles from the surface up to approximately 30 km with a much higher vertical resolution than the model in the stratosphere. Even if these type of measurements are greatly valuable, there are currently too sparse in time and space to help the characterization of the global transport in the IFS.

In this report, we are using only MIPAS retrievals for their coverage and their availability over time. The global coverage is a requirement as we are interested in evaluating the large scale stratospheric transport of the IFS. Note that Verma *et al.* (2016) compared IFS-based stratospheric methane profiles with both MIPAS and ACE-FTS. They found that the model and MIPAS retrievals comparison provides similar results than the model and ACE-FTS retrievals comparison, even if the first one is more robust due to the larger number of profiles available.

3.2 MIPAS retrievals

MIPAS is a Fourier transform spectrometer for the detection of limb emission spectra in the middle and upper atmosphere. It flew on board of ESA ENVISAT satellite between March 2002 and April 2012. MIPAS measured day and night, within the altitude range from 6 to 70 km. The measurements were performed from pole to pole, generating more than 1000 vertical profiles per day for 30 trace species, methane being among them.

In this document we are using the MIPAS level-2 data processed by the Institut für Meteorologie und Klimaforschung (IMK), which is complemented by the component of non-local thermodynamic equilibrium (non-LTE) treatment from the Instituto de Astrofísica de Andalucía (IAA). These IMK/IAA MIPAS level-2 data are part of the Climate Change Initiative (CCI, `www.esa-ghg-cci.org`). The used version of the product is either 21, 224 or 225 depending on the year and month. We selected the data only between 13 and 50 km as advised in the product documentation. We also removed the profiles for which the visibility flag was 0 and the levels where the absolute value of the diagonal element of averaging

kernel matrix was smaller than 0.03.

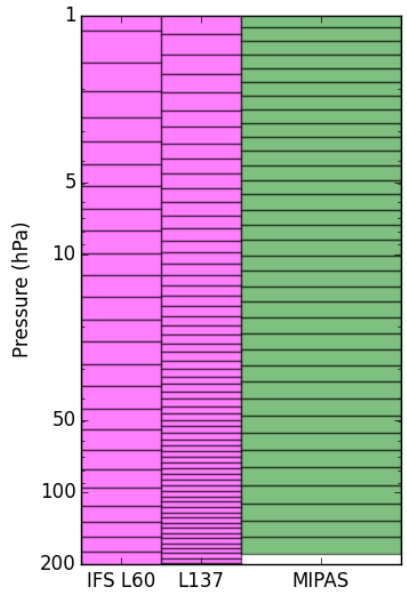

Figure 3: Vertical resolution of the IFS (left, magenta) and of MIPAS (right, green).

Figure 3 presents the vertical resolution of the IFS (60 & 137 levels) and the vertical resolution of MIPAS retrievals grid. The model 60 levels grid has a similar resolution than MIPAS retrieved grid in the UTLS. The size of the model grid box increases with altitude and above about 100 hPa it starts to be larger than that of MIPAS. At 1 hPa, the model layer is about 2.5 times larger than the vertical layer of MIPAS. For the 137 levels configuration, the model resolution is about 3 times higher than MIPAS resolution in the UTLS. At about 5 hPa both resolutions are similar. Higher in the stratosphere, at 1 hPa, the model resolution is about 1.5 times coarser that MIPAS resolution.

In this document, we performed the vertical interpolation from the model vertical grid toward MIPAS vertical grid and back (see sec. 5 for more information). Therefore the vertical resolution of the comparison will be, for each vertical level, on the coarser vertical grid between MIPAS and the model.

The size of the vertical layers being of the same order, we believe that the representativity error is small when performing the vertical interpolation from one grid to another. The error will be nevertheless larger above 5 hPa when using the 60 levels model grid.

4 Atmospheric methane modelling

As part of CAMS, atmospheric tracers were added to the IFS. In this document, we only detail the implementation related to methane. Methane mass mixing ratio is directly transported within the IFS as a tracer and it is affected by surface fluxes and chemistry. Here, we are using two versions of the chemical component:

1. IFS-CH_4-LR : the chemical methane tropospheric and stratospheric sinks are computed from monthly climatological fields of chemical loss rates (LR) from Bergamaschi *et al.* (2009) rather than computed from chemical mechanism. These climatological loss rates fields are based on OH fields optimised with methyl chloroform using the TM5 model (Krol *et al.*, 2005) and prescribed concentrations of the stratospheric radicals using the 2-D photochemical Max-Planck-Institute model. For more details on the implementation, the reader is referred to Massart *et al.* (2014).

2. IFS-CH_4-TS : an extensive combination of tropospheric (T) chemistry based on the CB05 mechanism (Yarwood *et al.*, 2005) and stratospheric (S) chemistry derived from the Belgian Assimilation System for Chemical ObsErvations (BASCOE) system (Errera *et al.*, 2008). For more details on the implementation of these chemical schemes in the IFS and on the merging procedure for the tropospheric and stratospheric chemistry, the reader is referred to Huijnen *et al.* (2016).

4.1 Loss rate (LR) configuration

For the IFS-CH_4-LR configuration, we are presenting here only cyclic hindcasts. Methane evolves alongside the other model variables during a 24 h forecast. All model variables but methane are updated after 24 h with the operational analysis, therefore benefiting from the assimilation of all the operational observations within the IFS 4DVar assimilation system. In the meantime, the CH_4 mass mixing ratio is cycled using the 24 h forecast as the initial condition for the next forecast. See Agustí-Panareda *et al.* (2014) for more details on the cycling forecast. We ran this configuration with various horizontal and vertical resolutions, but we mainly present here results from the TL255L137 grid (about 80 km$\times$80 km horizontal resolution and 137 vertical levels from the surface up to 0.01 hPa). Methane fluxes are prescribed using inventory and climatological data sets. The anthropogenic fluxes are from the EDGAR 4.2 database. The wetland fluxes are from the Kaplan climatology described in Bergamaschi *et al.* (2009). The biomass burning emissions are from the CAMS GFAS data set. The other sources/sinks include wild animals, termites, oceans and a soil sink. They are described in more detail in Massart *et al.* (2014).

4.2 Tropospheric-stratospheric (TS) configuration

For the IFS-CH_4-TS configuration, we are presenting here relaxation hindcasts (Huijnen *et al.*, 2016). In these runs the meteorological fields are relaxed towards the 6 hourly analysis from the ERA interim data set, which differs from the forcing of the previous configuration (operational analysis). This procedure allows to save computational time for long runs without impacting significantly the atmospheric composition compared to a cyclic 24 h forecast. Indeed, the relaxation runs are constrained by an analysis at a higher frequency (6 h versus 24 h) but the forcing is less rigid. This configuration runs on ERA interim's grid, a TL255L60 grid (horizontal resolution of about 80 km$\times$80 km and 60 levels from the surface up to 0.1 hPa). In this configuration, no CH_4 surfaces fluxes are used. Instead a climatology of surfaces values based on situ-observations is used to ensure a realistic boundary condition for CH_4.

4.3 Previous evaluation of the configurations

The methane parametrisation of Monge-Sanz *et al.* (2013) was implemented in two chemistry transport models (CTMs) and in the IFS. Simulated methane profiles were compared to HAOLE data for the year 2000. The yearly averaged profiles show an underestimation of methane in the IFS around 20 hPa at high latitudes, both compared to the methane profiles from the CTMs and from HALOE. One possible candidate that could explain the difference between the CTMs and the IFS is the treatment of the vertical motion. The CTMs obtain it from the divergence of the horizontal winds, while the IFS use its own instantaneous vertical wind velocity.

Huijnen *et al.* (2016) compared the simulated stratospheric profiles from the IFS-CH_4-TS configuration with ACE-FTS profiles for September-October-November 2009. They found a negative bias of IFS-CH_4-TS CH_4 in the lower stratosphere at all latitudes. In the middle stratosphere, between 20 hPa and 50 hPa, the bias is positive in the southern hemisphere and negative at high latitudes north. It is worth noting that they also used the BASCOE CTM that shares the same stratospheric chemistry than the IFS-CH_4-TS configuration. They forced BASCOE with the same dynamical fields (temperature, pressure and wind fields) as used in the IFS-CH_4-TS simulation. The comparison between the CTM and ACE-FTS profiles show that the bias is lower for BASCOE in the middle stratosphere than the bias of IFS-CH_4-TS . Like in Monge-Sanz *et al.* (2013), the differences between the CTM and the IFS could indicate a possible issue with the transport in the IFS.

Verma *et al.* (2016) compared stratospheric methane profiles of the IFS-CH_4-LR configuration with both MIPAS and ACE-FTS profiles for September-October-November 2010. They found similar results as from Huijnen *et al.* (2016) despite that the comparison was carried on a different year and a different configuration. This indicates a consistent error in the IFS transport. Moreover, they found that the comparison between IFS-CH_4-LR and MIPAS provides similar results than the comparison between IFS-CH_4-LR and ACE-FTS.

5 Model-MIPAS comparison methodology

MIPAS data are available between March 2002 and April 2012. When methane simulations are available during this period, we can directly compare them with MIPAS retrievals. When methane simulations are outside this period, a solution would be to use a MIPAS climatology instead. This is not the case for this document but this possibility is discussed in the appendix A (page 16).

In order to directly compare methane simulations with MIPAS methane retrieved profiles, we first extract the 3D simulated methane fields at their native resolution and with a 3-hourly time step. For each MIPAS methane profile, we extract the closest model profile on the grid and in time. This model profile $\boldsymbol{x}$ is interpolated towards $\boldsymbol{x}_m$ into the MIPAS vertical grid, using the weighting matrix $\boldsymbol{W}$,

$$\boldsymbol{x}_m = \boldsymbol{W}\boldsymbol{x}\,. \tag{1}$$

The averaging kernel is applied to the model interpolated profile $\boldsymbol{x}_m$ on MIPAS vertical grid,

$$\tilde{\boldsymbol{x}}_m = \boldsymbol{A}\boldsymbol{x}_m + (\boldsymbol{I}-\boldsymbol{A})\boldsymbol{x}_a\,, \tag{2}$$

where $\tilde{\boldsymbol{x}}_m$ is the smoothed model profile, $\boldsymbol{A}$ is the MIPAS averaging kernel matrix, $\boldsymbol{I}$ is the identity matrix, and $\boldsymbol{x}_a$ is the a priori profile. Note that for the used version of MIPAS data, the a priori profile is null.

The inverse operation, to map the smoothed model profile $\tilde{\boldsymbol{x}}_m$ from the MIPAS vertical grid to $\tilde{\boldsymbol{x}}$ on the model vertical grid, is executed with the weighting matrix $\boldsymbol{V}$,

$$\tilde{\boldsymbol{x}} = \boldsymbol{V}\tilde{\boldsymbol{x}}_m\,. \tag{3}$$

The choice of the inverse weight is not unique. We compute it with

$$\boldsymbol{V} = \left(\boldsymbol{W}^T\boldsymbol{W}\right)^{-1}\boldsymbol{W}^T\,, \tag{4}$$

which satisfies $\boldsymbol{V}\boldsymbol{W} = \boldsymbol{I}$.

Figure 4 presents some random examples of the smoothing process using the averaging kernel matrix $\boldsymbol{A}$ of Eq. (2). Samples #1 and #2 show that when the model profile is already smooth, the extra smoothing from the averaging kernel does not impact much the model profile (Figs. 4a and b). The last three samples show that when the model profile is less smooth, the extra smoothing from the averaging kernel also has a small impact on the model profile (Figs. 4c to e). Overall the differences between the smoothed model profile and the raw model profile are small compared to the difference between the model profile and MIPAS profile.

Every MIPAS methane retrieved profile and the co-located smooth model profile are interpolated on a 60 levels or 137 levels vertical grid (depending on the model resolution) based on IFS 60 levels or 137 levels respectively computed from a reference surface pressure of 1013.25 hPa. Then the difference between

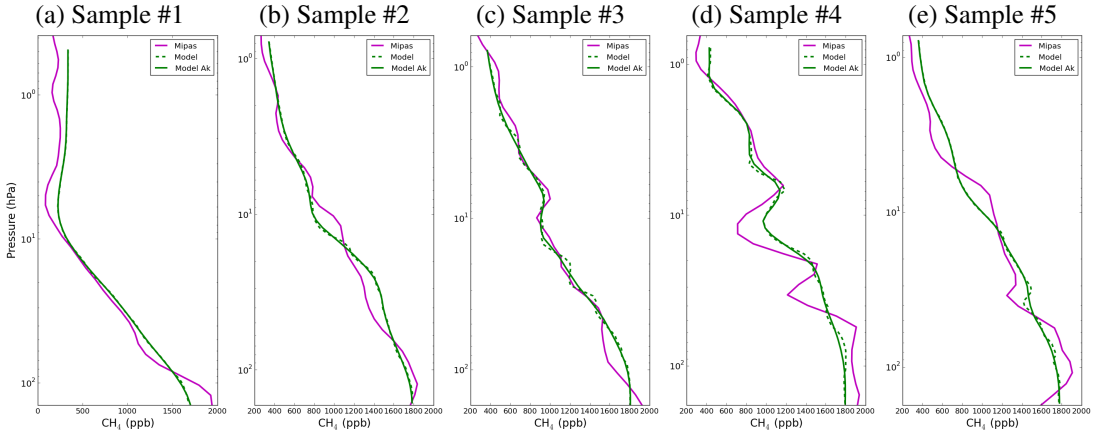

Figure 4: Examples of randomly chosen co-located MIPAS (magenta) and model (green) CH_4 profiles (in ppb). For the model, the dotted line is the raw model profile while the full line is the model profile smoothed by MIPAS averaging kernel.

MIPAS methane retrieved profile and the co-located smooth model profile is computed on this vertical grid. All the profiles of difference for a given month are then gridded horizontally on a regular $4^\circ \times 4^\circ$ grid. From this, we eventually compute the monthly mean. First results showed that the differences were mostly zonal (not shown). We therefore computed the zonal mean of the monthly mean. We also present in this document the monthly and zonal mean profiles for five latitude bands obtained by averaging all the monthly and zonal mean profiles in (i) the northern hemispheric (NH) high latitudes ($> 60^\circ N$), (ii) the NH mid-latitudes (between $60^\circ N$ and $30^\circ N$), (iii) the tropics (between $30^\circ N$ and $30^\circ S$), (iv) the southern hemispheric (SH) mid-latitudes (between $30^\circ S$ and $60^\circ S$) and (v) the SH high latitudes ($< 60^\circ S$).

Figures 5a and b illustrate the monthly and zonal means of the differences between model profiles and MIPAS profiles on a 137 level grid while using or not the averaging kernel of Eq. 2. First of all, this confirms that the usage of the averaging kernel makes little difference in the interpretation of the model bias against MIPAS, especially when the differences are averaged over a month and over the longitudes. Then the model bias against MIPAS is a large scale bias in the vertical and in the horizontal which justifies the choice of the horizontal regular $4^\circ \times 4^\circ$ grid for averaging the differences. Similarly, the difference between the MIPAS vertical resolution of the retrieved profiles and the model grids is not an issue.

6 IFS methane simulation versus MIPAS

The IFS-CH_4-TS configuration is much more computationally expensive than the IFS-CH_4-LR configuration. We decided in this document not to re-run any IFS-CH_4-TS experiment. Instead we use the experiment ran for the study of Huijnen *et al.* (2016) for which methane fields are available from May 2008 to December 2010 and based on the IFS cycle CY42r1.

In order to compare the two chemical components of the IFS for methane, we started the IFS-CH_4-LR hindcast with the same IFS cycle and from the same date as for the IFS-CH_4-TS configuration (1 May 2008) but we continued it until end of April 2012, last month when MIPAS data are available.

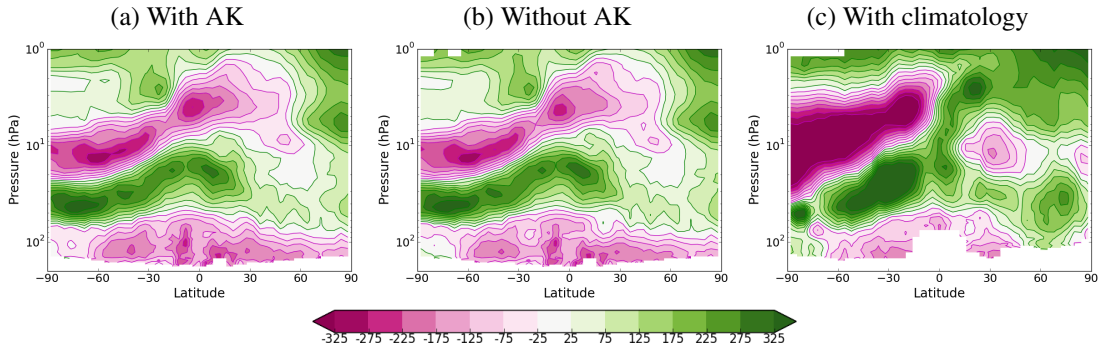

Figure 5: Example of monthly and zonal means CH_4 difference (in ppb) between model and MIPAS data (a) using MIPAS averaging kernel to smooth the model profile, (b) without using MIPAS averaging kernel and (c) using MIPAS climatology (2002-2012). The differences are computed for December 2010: green when the model has higher values than MIPAS and magenta for the opposite.

6.1 IFS-CH_4-LR versus MIPAS

Simulated methane concentrations from the IFS-CH_4-LR configuration tend to have lower values than the ones from MIPAS retrievals in the UTLS for all seasons and all latitudes (Figs. 6b, 7b and 8).

To better understand this difference, we investigated the sensitivity of the simulated methane in the UTLS with respect to some aspects of the physics parametrisation. We first ran some experiments with different values for the parameters of the vertical diffusion parametrisation implemented in the IFS (Chapter 3 of ECMWF (2016)). We did the same with the parameters of the non-orographic gravity waves parametrisation (Chapter 5 of ECMWF (2016)). The model bias with respect to MIPAS showed very low sensitivity to the configuration of both of them in the UTLS region and elsewhere (not shown). The large model bias in the UTLS could therefore not be explained alone by an inaccurate mixing in the stratosphere–troposphere exchange.

The methane chemistry not being very active in the UTLS (as discussed in sec. 2), the negative difference between IFS-CH_4-LR and MIPAS is probably the consequence of an underestimation in the tropospheric methane that propagates upstream. There is indeed evidence of an underestimation of the methane tropospheric column from the IFS-CH_4-LR configuration of about 35 ppb in average when compared to in-situ measurements sensitive to the lower troposphere (see Appendix B). The regional variability of the underestimation is less than 5 ppb, which means that the underestimation is well spread globally. It is likely associated with surface fluxes error (iv).

Around 10 hPa the model underestimates the methane concentration at high latitudes of the summer hemisphere, especially in the southern hemisphere (Fig. 8a). This is a region and a season where and when the methane loss rate is the highest as discussed in sec. 2. The underestimation is presumably due to errors in the methane chemistry (ii). This methane-poor air-mass then descents during the winter with the breaking of the planetary waves in the surf zone (Fig. 6b). This could help the underestimation in the lower stratosphere.

The model underestimation around 10 hPa at high latitudes is also associated with a model overestimation at the same altitude in the tropics (Fig. 7b). This could indicate that the horizontal mixing is too weak. A stronger horizontal mixing would indeed decrease the methane concentration in the tropics and increase it at higher latitudes.

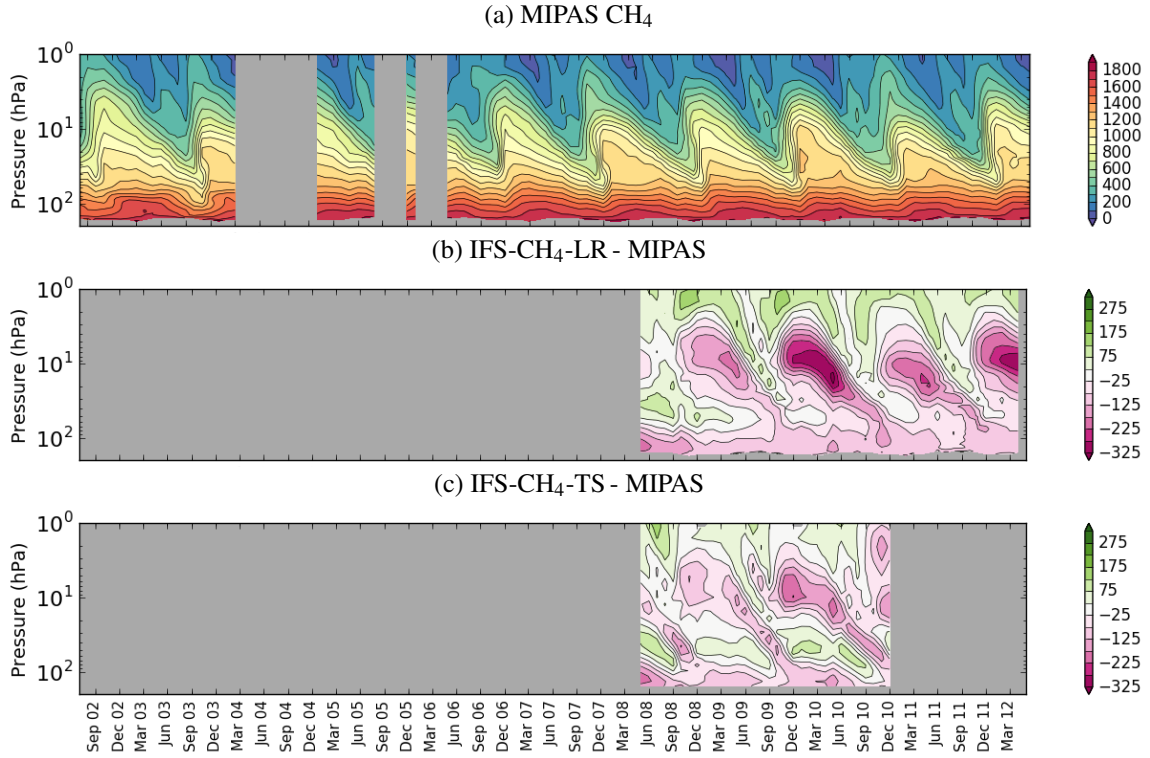

Figure 6: Time series of zonal and monthly mean methane profiles (in ppb) over the southern hemispheric high latitudes ($< 60°S$): (a) from MIPAS, (b) from IFS-CH_4-LR minus MIPAS and (c) from IFS-CH_4-TS minus MIPAS. For (b) and (c): green is when the model has higher values than MIPAS and magenta is for the opposite.

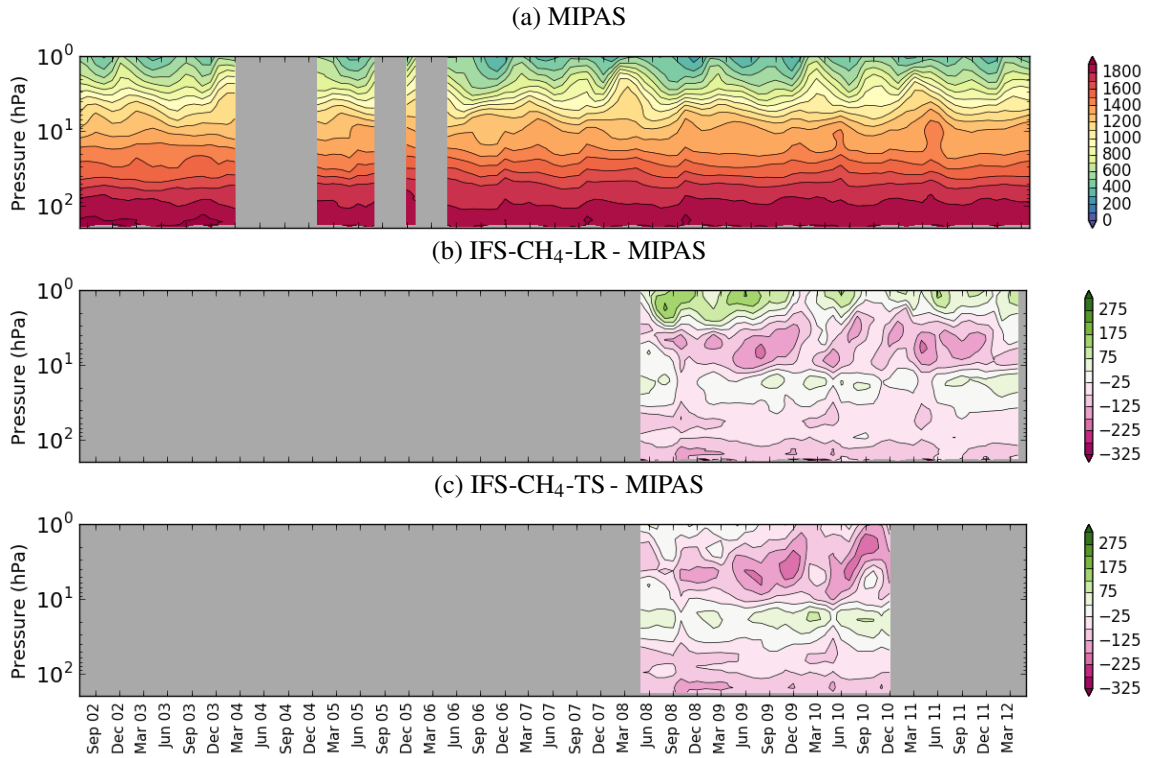

Figure 7: Same as Fig. 6 but for the tropics (between $30°N$ and $30°S$).

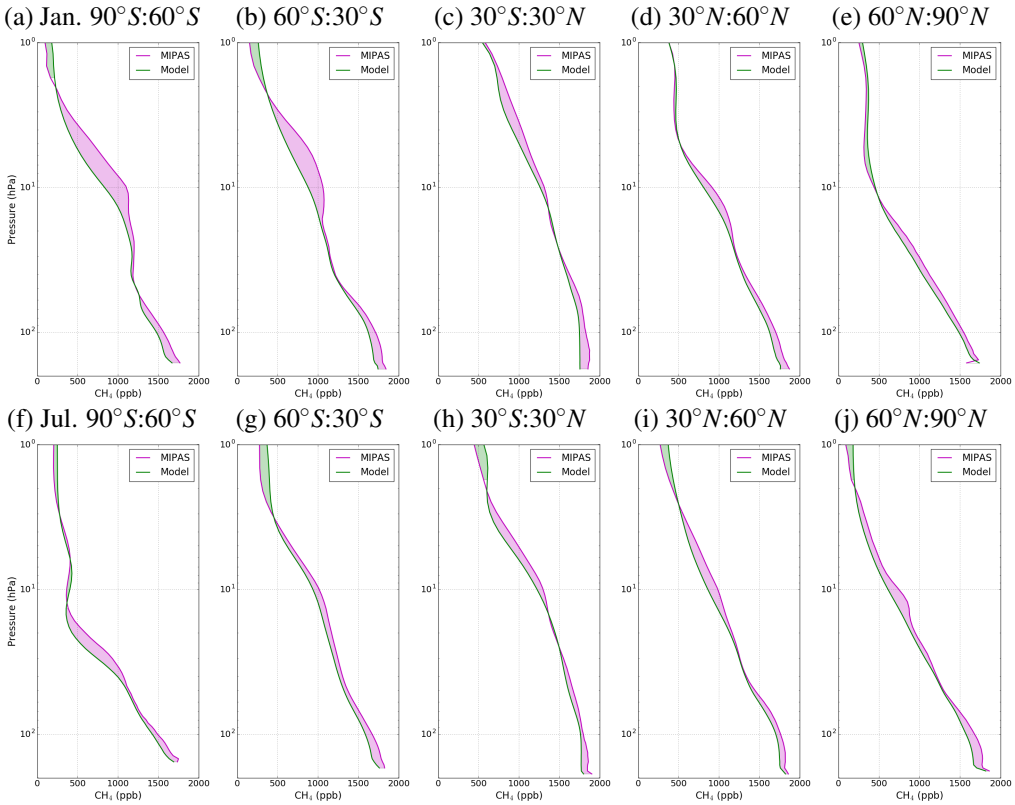

Figure 8: Monthly and zonal average methane profiles (in ppb) from the IFS-CH_4-LR experiment (green) and from MIPAS (magenta). Top: January 2010, bottom: July 2010. From left to right: latitude bands. The green shade is when model is higher than MIPAS and the magenta shade is for the opposite.

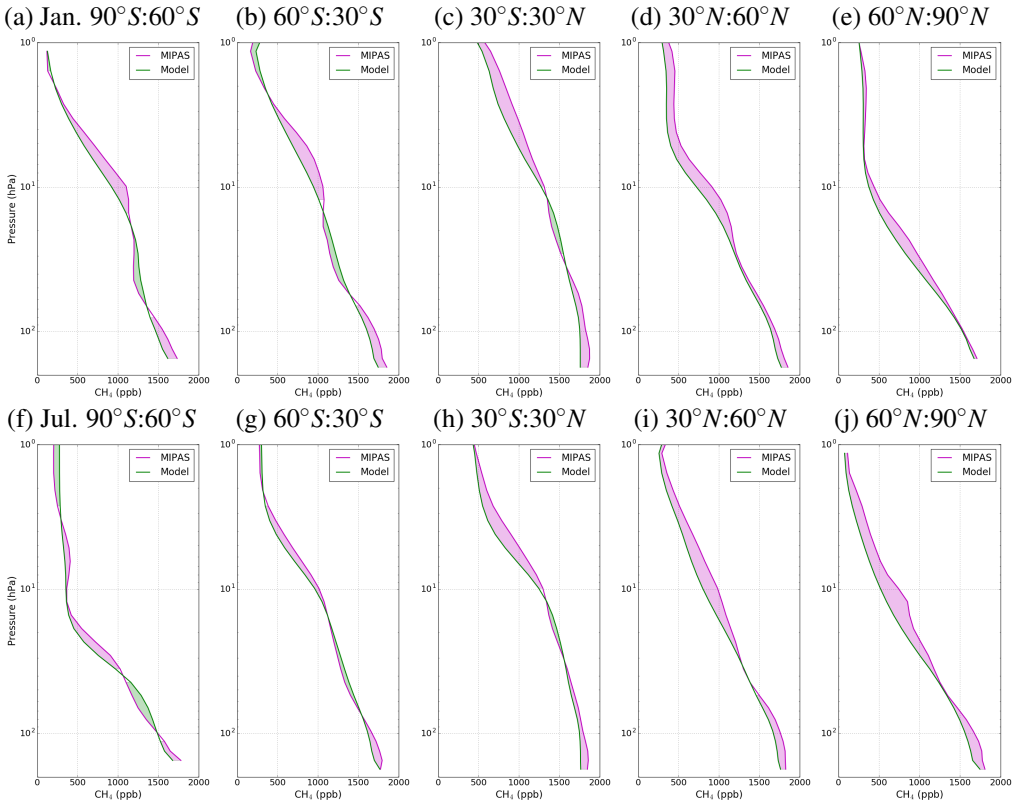

Figure 9: Same as Fig.8 but for the IFS-CH_4-TS

6.2 IFS-CH_4-TS versus MIPAS

The IFS-CH_4-TS configuration provides methane concentrations with similar characteristics than the ones provided by the previous configuration when compared against MIPAS retrievals. For example, the monthly mean methane profiles from the two configurations have similar biases with respect to MIPAS retrieved monthly mean profiles for January and July 2010, and for all latitude bands (Figs. 8 and 9). The model underestimation in the lower stratosphere is nevertheless sightly less than for the IFS-CH_4-LR configuration. This improvement could come from the difference in the treatment of the surface fluxes and of the chemistry.

In the middle and upper stratosphere, again the two configurations produce methane concentration with similar differences against MIPAS retrievals. There is nevertheless a slightly better fit with MIPAS retrievals for the IFS-CH_4-TS configuration (Fig. 6 and 7). When the chemical methane loss is large at high latitudes in the summer hemisphere, the underestimation is similar in both configuration despite having different chemical schemes. The chemistry could not be the only source of error there. The downward transport from the upper stratosphere during the winter could be too strong, leading to a deficit for the next summer.

The similar structure and amplitude of the differences against MIPAS retrievals for the two configurations means that the vertical resolution (60 versus 137 vertical levels), the forcing (ERA interim versus operational analysis) or the chemical scheme (extensive versus simplified) are not the main drivers behind the stratospheric methane bias in the model. The main common feature between the two configurations is the numerical model that transports methane.

6.3 Impact of the initial condition

From the IFS-CH_4-LR model-MIPAS differences, we computed the monthly mean difference for December 2010 on the horizontal regular $4^\circ \times 4^\circ$ grid. We removed this three dimensional methane monthly mean difference from the initial condition for 1 December 2010 up to 1 hPa. This new field is used as a new initial condition that is closer to the MIPAS data. From this new stratospheric methane initial condition, we ran the model for one year in the same condition as IFS-CH_4-LR run.

Figure 10 presents the monthly and zonal difference between the methane concentration from this new simulation and MIPAS retrievals. As expected, the mean difference for the first month (December 2010) is low compared to the differences found with the IFS-CH_4-LR experiment (Fig. 10a). Month after month, the difference increases and the patterns in the model-MIPAS difference become more and more similar to the ones of the reference experiment. It takes about six months for the differences to be almost the same (not shown). This means that the difference we found in the methane concentration between the model and MIPAS retrievals is not related to a bias in the stratospheric initial condition.

The time evolution of the difference could nevertheless help understanding the mechanism behind them. During the first months, the patterns of the difference seem to develop in three regions. The first region is the tropical UTLS and the underestimation spreads horizontally with time. The second region is the mid and upper tropical stratosphere, where a tri-pole pattern is forming. The last region is the high latitude south around 20 hPa were the underestimation is growing until May and which may feed the two other underestimation patterns. A similar negative pattern then starts growing at high latitude in the northern hemisphere.

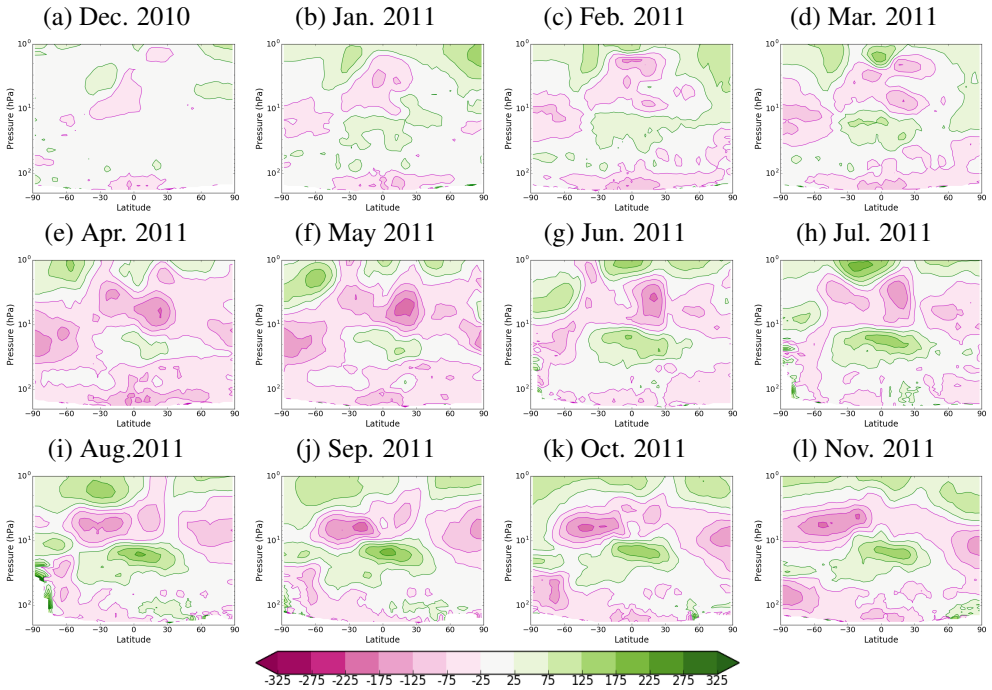

Figure 10: Monthly and zonal means of the methane difference (in ppb) between the IFS-CH_4-LR configuration with the bias corrected stratospheric initial condition and the MIPAS data: green when the hindcast has higher values than MIPAS and magenta for the opposite. The vertical coordinate is the pressure, between 200 hPa and 1 hPa.

7 Conclusions

In this document, we have studied the stratospheric methane simulated by the IFS using recent development from the Copernicus Atmosphere Monitoring Service (CAMS). We have used two configurations of methane chemistry: 1. IFS-CH_4-LR which which uses pre-defined methane loss rates rather than a chemical mechanism and 2. IFS-CH_4-TS which is based on a combination of a comprehensive tropospheric chemical mechanism and a comprehensive stratospheric one. We presented mainly the two configurations in forecast mode with the same horizontal resolution (TL255 or about 80 km $\times$ 80 km) but with two different vertical resolutions: 137 levels for IFS-CH_4-LR and 60 levels for IFS-CH_4-TS and two different forcings: operational analysis for IFS-CH_4-LR and ERA interim for IFS-CH_4-TS . The simulation period spans from May 2008 to April 2012 for IFS-CH_4-LR and to from May 2008 December 2010 for IFS-CH_4-TS with the IFS cycle CY42r1.

We compared the stratospheric methane profiles from the two simulations with MIPAS retrieved methane profiles from the Institut für Meteorologie und Klimaforschung (IMK), and the Instituto de Astrofísica de Andalucía (IAA). Despite some important differences between the two configurations that should have major impacts in the distribution of methane, they both present the same main features:

1. an underestimation of methane concentration in the upper troposphere lower stratosphere (UTLS) region for all latitudes and all months,

2. a large underestimation around 20 hPa particularly strong in the summer hemisphere at high latitude south, and

3. a small overestimation in-between, larger in the southern hemisphere and for the IFS-CH_4-TS simulation.

These biases could be linked with: (i) IFS transport error, (ii) simplified methane chemistry, (iii) initial condition of the simulation, (iv) surface fluxes error and (v) representativity error in the comparison.

We ran the IFS-CH_4-LR configuration removing the initial bias. This simulation started to present similar biases as for the reference simulation when compared to MIPAS retrieved profiles after less than 6 months. The initial condition (iii) is therefore not a candidate to explain the bias. Even if the two configurations (IFS-CH_4-LR and IFS-CH_4-TS) have two different ways of treating surface fluxes, they both underestimate the tropospheric amount of methane. This could come from surface fluxes error (iv) or wrong mixing (i) at the tropopause that acts as a barrier in the exchange between the troposphere and the stratosphere.

To better understand the impact of the transport on the bias, we also ran the IFS-CH_4-LR with 60 levels and with 137 levels on a TL1279 horizontal grid (about 14 km$\times$14 km). The results are not presented here, but the 60 levels configuration presented similar biases in shape as for the 137 levels configuration but with higher values. The TL1279 configuration provided similar biases in shape and amplitude as the TL255 configuration. These results plus the fact that the IFS-CH_4-LR and IFS-CH_4-TS presented configurations are using two different forcings (operational analysis and ERA interim) means that the the dominant part of the model methane bias is not resolution dependent or forcing dependent. Note that even if the different forcing is used, it is still the same model.

Another important result is that when Huijnen *et al.* (2016) forced BASCOE with the same dynamical fields (temperature, pressure and wind fields) and same methane chemistry as used in the IFS-CH_4-TS simulation, the bias 3 is lower for BASCOE than for IFS-CH_4-TS in the middle stratosphere (compared to ACE-FTS retrieved profiles). Similarly, when Monge-Sanz *et al.* (2013) compared another methane parametrisation in IFS with HALOE data, a similar bias is found in the IFS. The bias with respect to HALOE is also larger than the bias of a CTM using the same methane parametrisation. This means that the model methane bias does probably not come from the dynamical fields but likely by the vertical transport (the CTM using different vertical velocities) or the horizontal mixing of the IFS.

We ran other simulations (not shown) with an improved semi-Lagrangian scheme (Filip Vana, personal communication) or with various adequate values for the parameters of the diffusion parametrisation or the non-orographic gravity wave parametrisation. For all of them, the model bias showed very low sensitivity to the changes.

Comparing as many as possible independent tracers, like methane, ozone, carbon monoxide or humidity, with relevant observations is the way forward to better understand and document the stratospheric transport in the IFS. This would help to assess consistency and help to separate the contribution of the different processes towards the model biases. This would provide some indication as to whether the transport errors originate in the troposphere (e.g. convection overshoots) or in the stratosphere (e.g. advection in Brewer-Dobson circulation), or if it is more a bidirectional mixing issue in the IFS semi-lagrangian due to limited vertical resolution where the vertical gradients are large.

Moreover, IFS methane simulations could be used to test new or revised parametrisations of IFS that would impact the stratospheric transport. The advantage of this approach is that we have 10 years of MIPAS stratospheric methane retrievals. On the other hand the measurements stopped definitely in 2012 which would limit the tests to past periods. We also demonstrated that using a MIPAS based stratospheric methane climatology is not adequate. The other alternative would be to use retrievals from ACE-FTS that is still flying. The difference would be that ACE-FTS retrievals are sparse compared to MIPAS ones and therefore the confidence on the bias would be reduced.

Acknowledgement

We would like to thank Inna Polichtchouk and Beatriz Monge-Sanz for their help on this report. In particular, Inna provided useful insights on the stratospheric transport and helped to better interpret your results especially regarding her own results from Polichtchouk *et al.* (2017). Beatriz helped linking this study with her previous findings (Monge-Sanz *et al.*, 2013). We would like to also thank Peter Bechtold for his help on the sensitivity experiments to the physics parametrisations.

Appendix A Using MIPAS climatology to assess the model bias

When the model methane simulations are outside the availability period of MIPAS data, one could think of using a climatology of MIPAS methane profiles instead of the closest MIPAS profile in time and space as we did sec. 5. In that case, because the smoothing by MIPAS averaging kernel does not change significantly the model-MIPAS comparison, there is no need to compute and use a climatology of MIPAS averaging kernel as a first approximation.

First of all, we have to study the variability of stratospheric methane. If the variability is large on time scales of months to years compared to the mean, then the climatology based on monthly mean will not be useful. We chose to estimate this variability using MIPAS retrievals. Note that the main version of the MIPAS retrieved products is the same for the whole studied period but not the sub-versions (from version 21, 224 to 225). Using this non homogeneous sample could have side effects on the computation of the variability and we did not examine this particular issue.

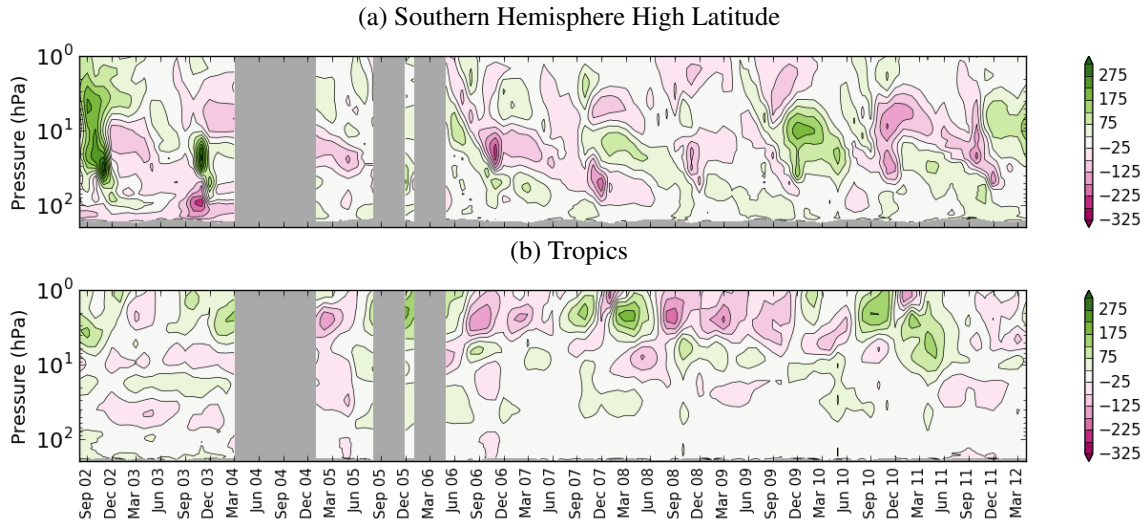

Figure A.1: Same as Fig. 6 but for MIPAS anomaly versus its own climatology: (a) SH and (b) Tropics.

For each month, we computed the climatology in averaging all the 2002-2012 MIPAS data for this particular month on a $4^\circ \times 4^\circ$ horizontal grid. Figure A.1 presents the time series of the differences between MIPAS retrieved profiles and the derived climatology for the southern hemisphere and the tropics. It shows first that there is not trend in the climatology that has to be removed. It also shows that the variability in time is large from one year to the next, especially of the southern hemisphere. For the tropics, the variability is smaller up to about 5 hPa which means that the climatology could be used mostly in that region and up to this pressure level.

For the month of December 2010, we compared the same simulated methane profiles as in sec. 5 with the new-build climatology of MIPAS methane profiles (Fig. 5c). The comparison confirms that using the climatology gives indeed a similar answer than a direct comparison in the tropics up to about 5 hPa. Elsewhere the comparison with MIPAS climatology allows to reproduce more or less the same general patterns of the bias as for the direct comparison but the amplitude is not right. Therefore, using methane MIPAS climatology to assess the model bias is not a suitable option.

Appendix B Comparison with TCCON in situ measurements

The Total Carbon Column Observing Network (TCCON) is a network of ground-based Fourier Transform Spectrometers recording direct solar spectra in the near infrared spectral region (http://tccon.ornl.gov/). The column-averaged dry-air mole fractions of CH_4 are retrieved from these spectra together with other chemical components of the atmosphere (Wunch *et al.*, 2011).

In the downloaded version GGG2014 of the data, 16 TCCON stations were providing data for the year 2011. We removed JPL 2011 (USA) and Tsukuba (Japan), as they are not background stations and are associated with significant representativity errors. This selection of the TCCON stations left 14 stations for the study (Table B.1).

Following Massart *et al.* (2016), we computed for each TCCON station k for $k \in [1,M]$ the mean (or bias) δ_k of the hourly averaged differences between the column-averaged dry-air mole fractions of CH_4 from the IFS-CH_4-LR simulation and from TCCON data. The number of hourly averaged differences are referred as N in Table B.1 for the year 2011. Additionally, we computed the the model offset δ and the station-to-station bias deviation σ:

$$\delta = \frac{1}{M}\sum_{k=1}^{M}\delta_k\,,$$

$$\sigma = \sqrt{\frac{1}{M-1}\sum_{k=1}^{M}[\delta_k-\delta]^2}\,.$$

Results are in Table B.1 for the year 2011 and for the IFS-CH_4-LR simulation. Only the yearly average is presented as there was no signal of a seasonal dependency of the model offset.

Table B.1: Mean difference of the column-averaged dry-air mole fractions of CH_4 (in ppb) between the IFS-CH_4-LR dataset and the average hourly TCCON data for the year 2011. Also shown are the mean bias and the deviation of the stations-to-station bias (in ppb) in the last two rows. The fourth column (N) is the number of data points used for computing the statistics while the second and third columns are the coordinates of the station (from North to South).

Site	Lat	Lon	N	Bias
Eureka	80.05	-86.42	74	-26.26
Sodankylä	67.37	26.63	834	-30.18
Białystok	53.23	23.02	340	-35.05
Bremen	53.10	8.85	151	-34.91
Karlsruhe	49.10	8.44	672	-33.53
Orléans	47.97	2.11	242	-36.36
Garmisch	47.48	11.06	702	-41.88
Park Falls	45.94	−90.27	836	-32.25
Lamont	36.60	−97.49	670	-39.61
Saga	33.24	130.29	83	-41.28
Darwin	−12.43	130.89	400	-28.13
Réunion Island)	−20.90	55.49	142	-33.02
Wollongong	−34.41	150.88	569	-32.61
Lauder	−45.05	169.68	1008	-31.46
Model Offset			14	-34.04
Bias Deviation			14	4.44

Appendix C Zonal mean differences

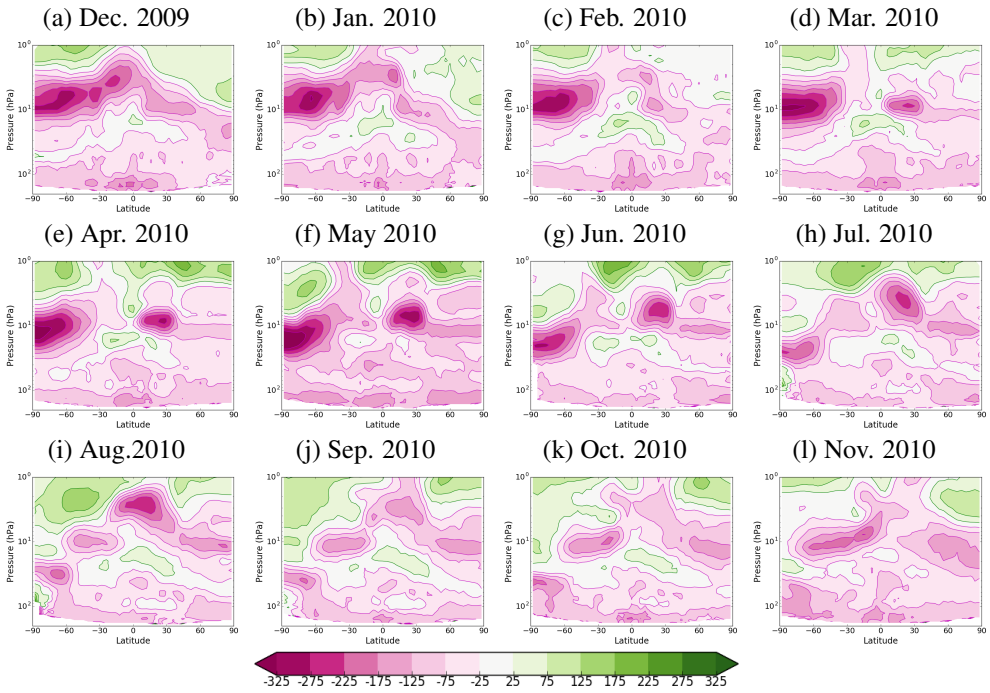

Figure C.2: Same as Fig. 10 but for the IFS-CH_4-LR configuration.

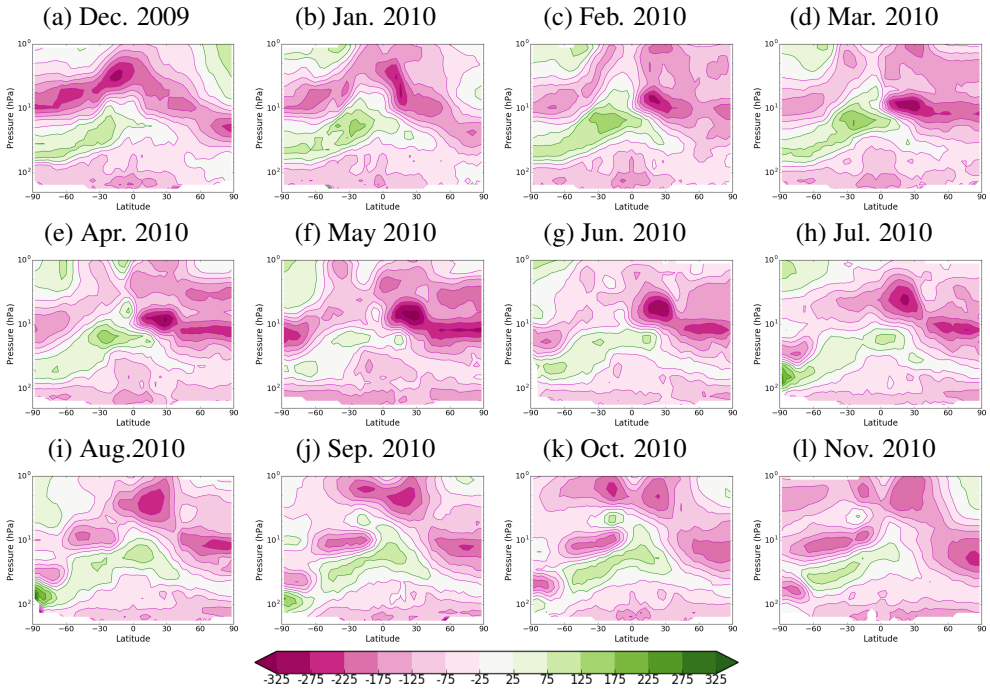

Figure C.3: Same as Fig.C.2 but for the IFS-CH_4-TS configuration.

References

Agustí-Panareda, A., S. Massart, F. Chevallier, S. Boussetta, G. Balsamo, A. Beljaars, P. Ciais, N. M. Deutscher, R. Engelen, L. Jones, R. Kivi, J.-D. Paris, V.-H. Peuch, V. Sherlock, A. T. Vermeulen, P. O. Wennberg, and D. Wunch, 2014: Forecasting global atmospheric CO_2. *Atmos. Chem. Phys.,* **14**(21), 11959–11983.

Bergamaschi, P., C. Frankenberg, J. F. Meirink, M. Krol, M. G. Villani, S. Houweling, F. Dentener, E. J. Dlugokencky, J. B. Miller, L. V. Gatti, A. Engel, , and I. Levin, 2009: Inverse modeling of global and regional CH4 emissions using SCIAMACHY satellite retrievals. *J. Geophys. Res. Atmos.,* **114**(D22301).

ECMWF, 2016: *Part IV: Physical Processes*. IFS Documentation CY43R1. ECMWF.

Errera, Q., F. Daerden, S. Chabrillat, J. C. Lambert, W. A. Lahoz, S. Viscardy, S. Bonjean, and D. Fonteyn, 2008: 4D-Var assimilation of MIPAS chemical observations: ozone and nitrogen dioxide analyses. *Atmos. Chem. Phys.,* **8**, 6169–6187.

Huijnen, V., J. Flemming, S. Chabrillat, Q. Errera, Y. Christophe, A.-M. Blechschmidt, A. Richter, and H. Eskes, 2016: C-IFS-CB05-BASCOE: Stratospheric Chemistry in the Integrated Forecasting System of ECMWF. *Geoscientific Model Development Discussions,* **2016**, 1–36.

Krol, M., S. Houweling, B. Bregman, M. van den Broek, A. Segers, P. van Velthoven, W. Peters, F. Dentener, and P. Bergamaschi, 2005: The two-way nested global chemistry-transport zoom model TM5: algorithm and applications. *Atmos. Chem. Phys.,* **5**, 417–432.

Massart, S., A. Agusti-Panareda, I. Aben, A. Butz, F. Chevallier, C. Crevosier, R. Engelen, C. Frankenberg, and O. Hasekamp, 2014: Assimilation of atmospheric methane products into the MACC-II system: from SCIAMACHY to TANSO and IASI. *Atmos. Chem. Phys.,* **14**(12), 6139–6158.

Massart, S., A. Agustí-Panareda, J. Heymann, M. Buchwitz, F. Chevallier, M. Reuter, M. Hilker, J. P. Burrows, N. M. Deutscher, D. G. Feist, F. Hase, R. Sussmann, F. Desmet, M. K. Dubey, D. W. T. Griffith, R. Kivi, C. Petri, M. Schneider, and V. A. Velazco, 2016: Ability of the 4-D-Var analysis of the GOSAT BESD XCO_2 retrievals to characterize atmospheric CO_2 at large and synoptic scales. *Atmos. Chem. Phys.,* **16**(3), 1653–1671.

Membrive, O., C. Crevoisier, C. Sweeney, F. Danis, A. Hertzog, A. Engel, H. Bönisch, and L. Picon, 2016: Aircore-HR: A high resolution column sampling to enhance the vertical description of CH_4 and CO_2. *Atmos Meas. Tech. Discuss.,* **2016**, 1–31.

Mohanakumar, K., 2008: *Stratosphere Troposphere Interactions. An Introduction*. Spinger.

Monge-Sanz, B. M., M. P. Chipperfield, A. Untch, J.-J. Morcrette, A. Rap, and A. J. Simmons, 2013: On the uses of a new linear scheme for stratospheric methane in global models: water source, transport tracer and radiative forcing. *Atmospheric Chemistry and Physics,* **13**(18), 9641–9660.

Polichtchouk, I., R. Hogan, T. Shepherd, P. Bechtold, T. Stockdale, S. Malardel, S.-J. Lock, and L. Magnusson, 2017. What influences the middle atmosphere circulation in the ifs? Technical Memorandum No. 809.

Verma, S., J. Marshall, M. Parrington, A. Agusti-Panareda, S. Massart, M. P. Chipperfield, C. Wilson, and C. Gerbig, 2016: Extending methane profiles from aircraft into the stratosphere for satellite total column validation: A comparative analysis of different data sources. *Atmos. Chem. Phys. Discuss.,* **2016**, 1–32.

Wunch, D., G. C. Toon, J.-F. L. Blavier, R. A. Washenfelder, J. Notholt, B. J. Connor, D. W. T. Griffith, V. Sherlock, and P. O. Wennberg, 2011: The Total Carbon Column Observing Network. *Philos. T. Roy. Soc. A,* **369**(1943), 2087–2112.

Yarwood, G., S. Rao, M. Yocke, and G. Whitten, 2005. Updates to the carbon bond chemical mechanism: CB05. Final report to the US EPA, EPA Report Number: RT-0400675, available at: www.camx.com.